Zahn, R., Comas, M.C., and Klaus, A. (Eds.), 1999
Proceedings of the Ocean Drilling Program, Scientific Results, Vol. 161

32. CARBON, SULFUR, AND OXYGEN ISOTOPE GEOCHEMISTRY OF INTERSTITIAL WATERS FROM THE WESTERN MEDITERRANEAN[1]

Michael E. Böttcher,[2,4] Stefano M. Bernasconi,[3] and Hans-Jürgen Brumsack[2]

ABSTRACT

Interstitial waters from six sites of the Western Mediterranean Basin (Sites 974–979) were analyzed for stable isotopes of dissolved sulfate ($\delta^{34}S$, $\delta^{18}O$), water ($\delta^{18}O$), and dissolved inorganic carbon (^{13}C), in addition to major and minor ions.

Sulfate reduction rates (as determined by modeling sulfate profiles) are positively related to bulk sedimentation rates, which indicates a higher burial of metabolizable organic matter with increasing sedimentation rate. Bacterial sulfate reduction in the deeper samples from Sites 974 and 978 is overprinted by a sulfate input from saline brines located at depth. Dissolution of gypsum within the section cored was found at Site 975. The concentration and sulfur isotopic composition of pore-water sulfate ($\delta^{34}S$ values up to +89‰ relative to the Vienna-Canyon Diablo troilite standard) are dominated by microbial organic matter oxidation with associated sulfate reduction. Therefore, most interstitial sulfate is enriched in ^{34}S with respect to modern Mediterranean seawater ($\delta^{34}S$ = +20.7‰; Site 973 surface seawater). Dissolved sulfate at Sites 974, 975, 977, and 979 is also enriched in ^{18}O with respect to Mediterranean seawater ($\delta^{18}O[SO_4^{2-}]$ = +9.4‰ relative to Standard Mean Ocean Water). The sulfur and oxygen isotopic compositions of dissolved residual sulfate are positively correlated to each other. Microbiologically mediated oxygen isotope exchange reactions lead to isotope shifts towards equilibrium between residual sulfate and interstitial H_2O with increasing degree of sulfate reduction. The results support the previous suggestion that $\delta^{18}O$–$\delta^{34}S$ relations of residual sulfate directly reflect sulfate reduction rates in marine sediments.

The depth profiles of the carbon isotopic composition of dissolved inorganic carbonate species ($\delta^{13}C$ values between –0.1‰ and –22.6‰ relative to the Vienna Peedee Belemnite standard) reflect the in situ degradation of organic matter via sulfate reduction, followed by the formation of methane via in situ fermentation of organic matter, and probably carbonate dissolution and precipitation.

INTRODUCTION

Interstitial waters from six sites of the Western Mediterranean Basin (Sites 974–979; Fig. 1) were retrieved during Leg 161 of the Ocean Drilling Program (ODP) and analyzed for stable isotopes of dissolved sulfate ($^{34}S/^{32}S$, $^{18}O/^{16}O$), water ($^{18}O/^{16}O$), and inorganic carbonate species ($^{13}C/^{12}C$), in addition to major and minor ions. Site 974 was drilled in the central Tyrrhenian Sea. Site 975 was located on the South Balearic Margin, between the Balearic Promontory (Menorca and Mallorca Islands) and the Algerian Basin. Sites 977 and 978 are situated in the Eastern Alboran Sea, and Sites 976 and 979 were drilled in the Western and Southern Alboran Sea, respectively (Comas, Zahn, Klaus, et al., 1996). The recovered sediments span a time interval from the Pleistocene to the Miocene (Comas, Zahn, Klaus, et al., 1996). Several sapropel layers with organic carbon contents up to 6.3% by weight (Comas, Zahn, Klaus, et al., 1996) were found at almost all sites and reflect periods of enhanced organic matter production and/or preservation.

Pore waters were retrieved from all sites drilled during Leg 161 to characterize the early and late diagenetic microbial degradation of organic matter within the sediment column and the influence of evaporites or brines at depth on the interstitial waters of the sediments.

SAMPLING AND ANALYTICAL METHODS

Interstitial water samples were squeezed from whole-were found at almost all whole-round samples immediately after retrieval of the core using the standard ODP titanium/stainless-steel squeezer (Manheim and Sayles, 1974). The retrieved pore waters were subsequently analyzed on board ship for salinity, pH, alkalinity, sulfate, chloride, lithium, potassium, sodium, calcium, magnesium, strontium, manganese, ammonium, phosphate, and silica using the methods described in Gieskes et al. (1991). Sulfur and oxygen isotope measurements of dissolved sulfate were determined on pore waters previously used for shipboard alkalinity determinations. Therefore, dissolved sulfide, if present, was removed from the aqueous solution. The sulfate was precipitated quantitatively as $BaSO_4$ by the addition of barium chloride, washed with deionized water, and dried at 110°C. Sulfur isotope ratios ($^{34}S/^{32}S$) of $BaSO_4$ were analyzed by combustion-isotope-ratio-monitoring mass spectrometry (C-irmMS) as described by Böttcher et al. (1998). About 0.4 mg $BaSO_4$ was combusted in an elemental analyzer (Carlo Erba EA 1108) connected to a Finnigan MAT 252 mass spectrometer via a Finnigan MAT Conflo II split interface. The liberated SO_2 gas was transported in a continuous stream of He (5.0 grade). Filtered samples for carbon isotopes of dissolved inorganic carbonate species and oxygen isotopes of water measurements were sealed in glass ampules immediately after recovery and stored in the dark. For carbon isotope determination of dissolved inorganic carbonate species, 1–2 mL of water was drawn with a syringe immediately after breaking the seal of the ampule. Then it was injected into a previously evacuated vacutainer containing 0.1 mL of 100% phosphoric acid. The evolved CO_2 was cryogenically purified on a vacuum line and measured using a Fisons-Optima mass spectrometer calibrated with the NBS-19 standard. The accuracy and precision of the method were determined by multiple measurements of a solution of

[1]Zahn, R., Comas, M.C., and Klaus, A. (Eds.), 1999. *Proc. ODP, Sci. Results*, 161: College Station, TX (Ocean Drilling Program).

[2]Institute of Chemistry and Biology of the Marine Environment (ICBM), Carl von Ossietzky University, P.O. Box 2503, D-26111 Oldenburg, Federal Republic of Germany.

[3]Geologisches Institut, ETH-Zentrum, CH-8092 Zürich, Switzerland.

[4]Present address: Department of Biogeochemistry, Max-Planck-Institute for Marine Microbiology, Celsiusstr.1, D-28359 Bremen, Federal Republic of Germany.
mboettch@mpi-bremen.de

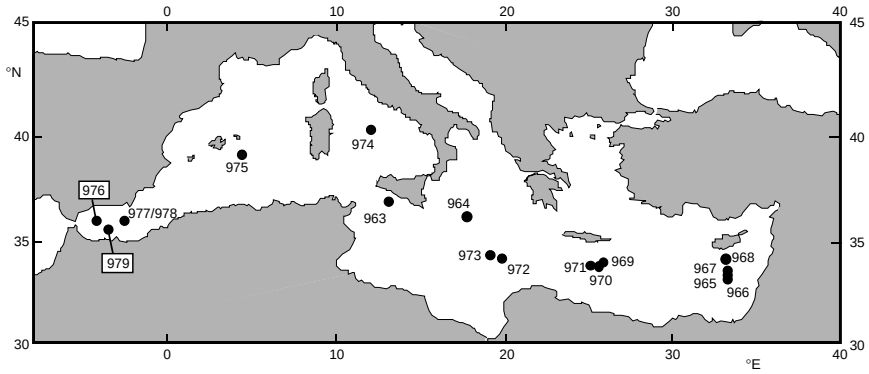

Figure 1. Outline map of the Mediterranean showing sites of Leg 160 (Sites 963–973) and Leg 161 (Sites 974–979).

sodium bicarbonate of known isotopic composition. Reproducibility of the method is ±0.3‰. Oxygen isotope measurements on water were conducted using an automated equilibration device with a reproducibility of ± 0.06‰. Oxygen isotope measurements on $BaSO_4$ were performed at the Marie Curie-Skolodowska University of Lublin, Poland, according to the method described by Mizutani (1971). Stable sulfur, oxygen, and carbon isotope ratios are presented using the δ-notation with respect to the Vienna-Canyon Diablo troilite standard (V-CDT), Vienna-Standard Mean Ocean Water (V-SMOW), and the Vienna-Peedee-Belemnite standard (V-PDB), respectively. A $\delta^{34}S$ value of +20.59‰ was obtained for the NBS-127 ($BaSO_4$) standard (Böttcher et al., 1997). The measured $\delta^{18}O$ value of +9.53‰ for NBS-127 agrees with the proposed value of +9.34 ± 0.32‰ (Gonfiantini et al., 1995).

RESULTS AND DISCUSSION

Sulfate Reduction

From the downcore variation of dissolved sulfate concentrations in the interstitial waters (Fig. 2), it is evident that most of the sites are characterized by more or less intense bacterial sulfate reduction. Even at those sites where the pore-water sulfate concentrations are comparable to those of modern Mediterranean seawater (~31 mM; surface seawater at Site 973; Böttcher et al., 1998), microbial activity using sulfate as the electron acceptor is observed from the sulfur isotopic trends of residual sulfate (see section on sulfur isotopes).

The reduction of dissolved sulfate is coupled to the availability of metabolizable organic matter in the sediments. Whereas sulfate reduction is essentially complete in the upper meters of Sites 976 and 977 (Table 1; Fig. 2), significant amounts of sulfate are present in the interstitial waters of all other sites. No influence of organic-rich layers (sapropels) in the sediment column on the pore-water sulfate profiles is observed. Sulfate reduction rates for the upper parts of the sediment sections of all sites except for 978 were calculated according to Canfield (1991) and are positively correlated to the bulk sedimentation rates (Fig. 3), which is consistent with higher preservation of metabolizable organic matter with increasing sedimentation rate (Berner, 1980). The results for the western Mediterranean (Leg 161; this study) compare well with those for the eastern Mediterranean (Leg 160; Böttcher et al., 1998). It should be noted that the sulfate reduction rates were determined by modeling the sulfate profiles (Canfield, 1991), which may depart from direct measurements derived from $^{35}SO_4^{2-}$ incubations.

The sulfate profiles at Sites 976 and 977, and probably Site 979, show a convex-up curvature (Fig. 2) which, together with the downward increase in alkalinity and dissolved ammonium (Comas, Zahn, Klaus, et al., 1996), indicate that sulfate reduction seems to be related to the microbial in situ degradation of organic matter and that upward diffusion of methane played no significant role in the upper part of the sedimentary column (Borowski et al., 1996). For Sites 974, 975, and 978, an increase in sulfate concentrations is found deeper downcore (Fig. 2). This is caused by a superimposition of bacterial sulfate reduction by a sulfate input from the dissolution of upper Miocene evaporites or the influence of saline brines located at depth. The upward sulfate flux from evaporitic brines is inferred from salinity and major-element variations of the interstitial waters from Sites 974 and 978 (Comas, Zahn, Klaus, et al., 1996). These brines may be paleofluid that had been trapped below the Pliocene–Pleistocene sediments or brines derived from salt dissolution (Comas, Zahn, Klaus, et al., 1996). Evaporite dissolution may have occurred in underlying strata or in distant Messinian salt deposits followed by large-scale fluid migration along permeable sediments to the investigated site (Comas, Zahn, Klaus, et al., 1996). At Sites 975 and 978, gypsum was found in the deeper sediment cores and the pore-water profiles provide evidence for the dissolution of calcium sulfates (Comas, Zahn, Klaus, et al., 1996; Bernasconi, Chap. 33, this volume).

Sulfur Isotopes

The microbial reduction of dissolved sulfate leads to a kinetic isotope effect and an enrichment of the lighter sulfur isotope, ^{32}S, in the formed hydrogen sulfide and a corresponding increase in the isotope composition of the residual sulfate (e.g., Chambers and Trudinger, 1979). Rayleigh fractionation evaluation of the residual sulfate data of Sites 975, 976, and 977, assuming closed system conditions with respect to dissolved sulfate (Hartmann and Nielsen, 1969; Sweeney and Kaplan, 1980), yields linear correlations (Fig. 4) and fractionation factors between 1.019 and 1.066. The values for Sites 976 and 977 are within the range observed experimentally for microbial sulfate reduction at low reaction rates (Chambers and Trudinger, 1979; Canfield and Teske, 1996; Rees, 1973). A contribution of sulfate diffusion from the sediment-water interface (i.e., SO_4^{2-} that is ^{34}S depleted relative to the residual pore-water sulfate) to the interstitial water sulfate pool would increase the calculated fractionation factors (Jørgensen, 1979). The calculated fractionation factor for the upper sediment column at Site 975 exceeds the experimentally observed range, which may be caused by a very low sulfate reduction rate.

A superimposition of bacterial sulfate reduction is found in the samples from Site 975 below ~47 meters below seafloor (mbsf) by a sulfate input from upper Miocene evaporites located at depth with a $\delta^{34}S$ value ~+23‰ (Table 2). The dissolution of sulfate minerals from evaporites does not lead to sulfur isotope fractionation (Böttcher and Usdowski, 1993). Therefore, late Miocene sulfates contribute to the sulfur isotopic composition of the interstitial sulfate with a $\delta^{34}S$ value of ~+23‰, in general agreement with the observed variation of $\delta^{34}S$ values at Site 975 (Fig. 2). Considering an enrichment of ^{34}S by ~+1.6‰ in the solid during crystallization of gypsum (Thode and Monster, 1965), the parent solution of Site 975 gypsum should have had an isotopic composition ~+21‰, which is similar to that of mod-

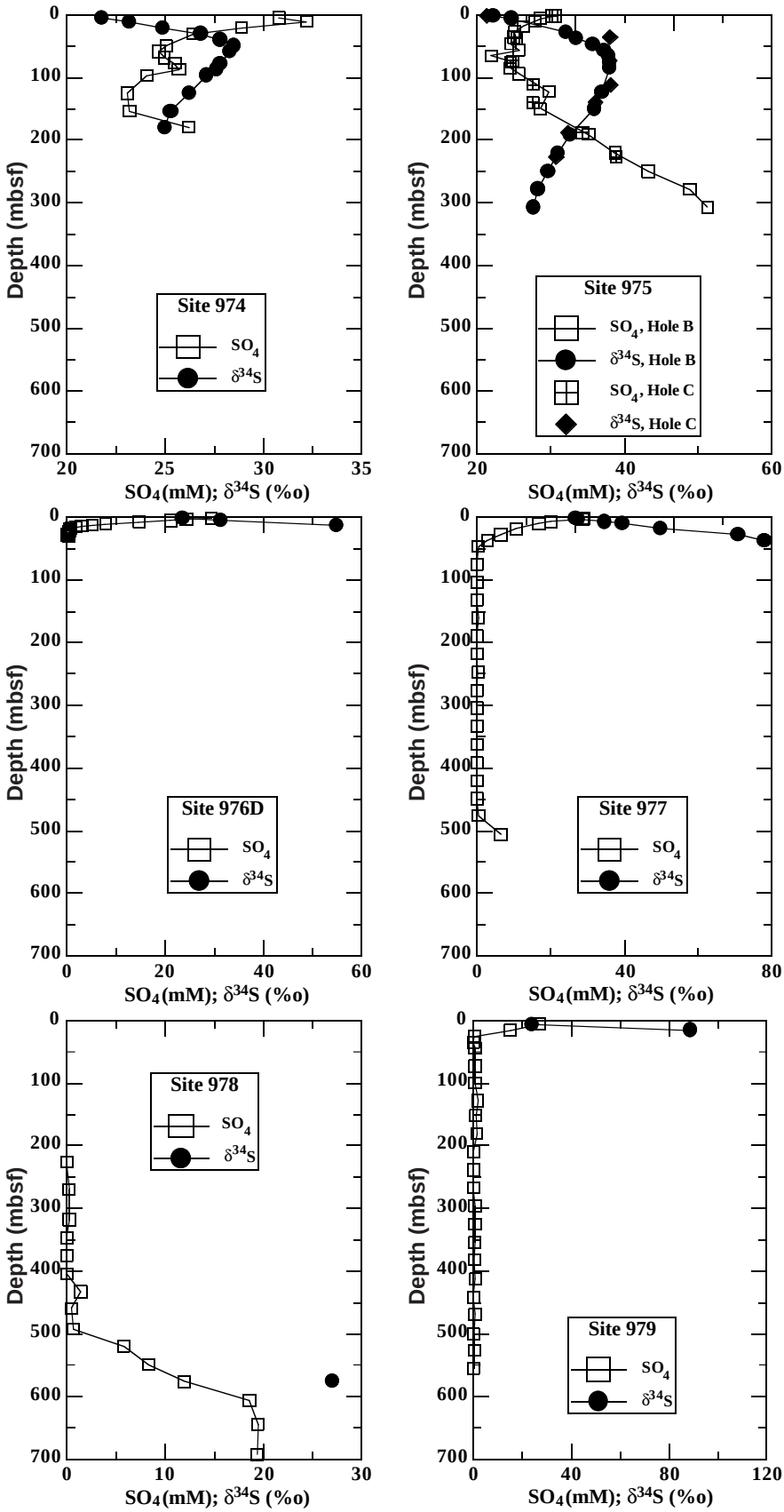

Figure 2. Pore-water sulfate concentration and $\delta^{34}S$ data vs. depth profiles from Sites 974 to 979.

Table 1. Stable sulfur and carbon isotopes in pore waters from Leg 161.

Core, section, interval (cm)	Depth (mbsf)	SO_4 (mM)	$\delta^{34}S$ (‰)	TA (mM)	$\delta^{13}C$ (‰)
161-974B-					
1H-3, 145-150	4.45	30.8	21.8	3.2	–4.86
2H-3, 145-150	10.95	32.2	23.2	3.2	–4.03
3H-3, 145-150	20.45	28.9	24.9	2.8	–6.26
4H-3, 145-150	29.95	26.4	26.8	2.6	–6.70
5H-3, 145-150	39.45	—	27.8	2.8	—
6H-3, 145-150	48.95	25.1	28.5	2.8	–5.35
7H-3, 145-150	58.16	24.7	28.3	3.0	—
8H-3, 135-140	67.85	25.0	—	3.0	–3.65
9H-3, 145-150	77.35	25.5	27.8	2.9	—
10H-3, 145-150	86.65	25.7	27.6	2.9	–3.67
11H-3, 145-150	96.45	24.1	27.1	3.0	—
14H-3, 145-150	124.95	23.1	26.2	2.4	—
17H-3, 145-150	153.45	23.2	25.3	2.0	–3.10
20X-3, 145-150	179.35	26.2	25.0	1.9	—
161-975B-					
1H-1, 145-150	1.45	30.7	22.2	3.3	–5.08
2H-1, 145-150	5.55	28.6	24.7	4.2	—
2H-4, 145-150	10.05	27.9	—	4.3	—
3H-3, 145-150	18.05	26.3	—	4.4	—
4H-3, 145-150	27.55	25.1	32.1	4.3	–6.39
5H-3, 145-150	37.05	25.4	33.5	4.5	—
6H-3, 145-150	46.55	24.6	35.7	4.3	—
7H-3, 145-150	56.05	25.7	37.2	4.3	–6.57
8H-3, 135-140	65.45	21.9	37.8	4.7	—
9H-3, 145-150	75.05	24.6	37.9	3.9	–5.34
10H-3, 145-150	84.55	24.5	37.9	3.8	—
11H-3, 145-150	94.05	25.7	—	3.7	–4.98
14H-3, 145-150	122.55	29.8	36.9	3.6	—
17X-2, 145-150	149.55	28.6	35.9	3.2	—
21X-3, 145-150	190.85	35.1	32.7	2.6	–5.03
24X-3, 145-150	220.35	38.7	31.0	2.3	—
27X-3, 145-150	249.25	43.2	29.7	2.0	—
30X-3, 145-150	278.05	48.9	28.3	1.5	—
33X-3, 145-150	306.85	51.3	27.7	1.4	–3.22
161-975C-					
1H-1, 145-150	1.45	30.2	21.3	3.6	—
5H-3, 145-150	35.35	25.0	38.0	4.3	—
9H-3, 145-150	73.35	24.9	37.9	3.8	—
13H-3, 145-150	111.35	27.6	38.1	3.6	—
16H-3, 145-150	139.85	27.6	36.0	3.4	—
21X-3, 145-150	187.85	34.3	32.4	2.6	—
25X-3, 145-150	226.15	38.8	30.8	2.1	—
161-976D-					
1H-1, 128-133	1.28	29.3	23.6	5.4	–10.71
2H-1, 145-150	2.95	24.2	—	8.3	—
2H-2, 145-150	4.45	21.2	31.3	11.9	–15.61
2H-4, 145-150	7.45	14.7	—	16.8	—
2H-6, 145-150	10.45	7.9	—	23.2	–17.79
3H-1, 145-150	12.45	5.2	55.0	24.3	—
3H-2, 145-150	13.95	3.0	—	25.8	–18.30
3H-3, 145-150	15.45	1.9	—	26.6	—
3H-4, 145-150	16.95	0.9	—	26.5	—
3H-5, 145-150	18.45	0.6	—	24.8	–18.29
3H-6, 145-150	19.95	—	—	23.5	—
3H-7, 145-150	20.45	—	—	22.5	–17.90
4H-1, 145-150	21.95	0.5	—	19.2	—
4H-2, 145-150	23.45	0.4	—	17.2	–18.49
4H-3, 145-150	24.95	—	—	15.5	—
4H-4,145-150	26.45	0	—	15.0	–19.09
4H-5, 145-150	27.95	0.1	—	14.4	—
4H-6, 145-150	29.45	0.3	—	13.8	–18.73
161-976C-					
4H-4, 145-150	30.95	—	—	14.1	—
5H-6, 145-150	43.45	—	—	12.6	–22.55
6H-4, 145-150	49.95	—	—	12.4	–21.99
7H-4, 145-150	59.45	—	—	13.4	—
8H-4, 145-150	68.95	—	—	13.2	–13.99
161-977A-					
1H-1, 145-150	1.45	28.9	26.9	5.6	–10.31
1H-2, 145-150	2.95	28.6	27.6	7.1	—
2H-2, 145-150	6.88	20.1	34.5	12.5	–15.79
2H-4, 145-150	9.88	16.8	39.4	14.4	—
3H-3, 145-150	17.95	10.7	49.7	15.1	–15.29
4H-3, 145-150	27.45	6.5	71.0	13.5	—
5H-3, 145-150	36.95	2.7	78.1	13.2	–17.63
6H-3, 145-150	46.45	0.3	—	—	–19.92
9H-3, 145-150	74.95	0	—	10.4	–10.32
12H-3, 145-150	103.45	0	—	10.9	–4.83
15H-3, 145-150	131.95	0	—	8.7	—
18X-3, 145-150	160.45	0.3	—	7.1	—
21X-3, 145-150	189.35	0	—	5.6	—
24X-3, 140-150	218.0	0	—	4.7	–3.33
27X-3, 140-150	247.0	0.2	—	4.1	—
30X-3, 140-150	275.8	0	—	3.7	–3.60
33X-3, 140-150	304.5	0	—	4.5	—
36X-3, 140-150	333.3	0	—	2.8	–5.64
39X-3, 140-150	362.6	0	—	2.5	—
42X-3, 140-150	391.1	0	—	1.9	–6.69
45X-3, 140-150	420.0	0	—	1.6	—
48X-3, 140-150	448.9	0	—	1.3	–7.74
51X-2, 140-150	476.2	0.4	—	1.4	—
54X-3, 140-150	506.5	6.5	—	—	–17.91
161-978A-					
41R-2, 135-150	575.65	11.9	27.1	1.04	—
161-979A-					
2H-3, 145-150	5.95	27.1	23.9	6.4	–11.13
3H-3, 145-150	15.45	15.2	88.9	15.4	—

Note: — = not determined.

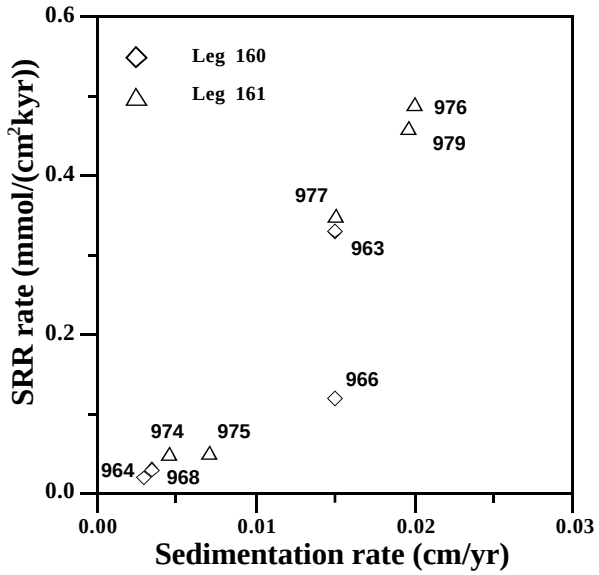

Figure 3. Variation of sulfate reduction rates (SRR) of selected sites from the western (Leg 161; this study) and eastern Mediterranean (Leg 160; Böttcher et al., 1998) as a function of the sedimentation rate.

ern Mediterranean seawater (Böttcher et al., 1998; De Lange et al., 1990), and the inferred variation of seawater isotopic composition within the last 10 Ma (Burdett et al., 1989). The sulfur isotopic composition of dissolved sulfate at 576 mbsf at Site 978 (+27.1‰; Table 1) demonstrates that Messinian calcium sulfates and/or saline brines were probably the source of the dissolved sulfate, and that minor microbial sulfate reduction occurred. Trapped late-stage evaporitic brines or brines derived from the dissolution of Messinian salts should contribute sulfate with a $\delta^{34}S$ value ~+23‰.

Figure 5 summarizes all measured sulfur isotope data as a function of the residual sulfate concentration and compares the results with some predicted general trends, which are, alone or in combination, responsible for the observed variations in the interstitial waters from Leg 161. From a comparison of the analyzed pore waters with these trends, it is evident that the dominant processes influencing the relationships between concentration and sulfur isotopic composition of residual dissolved sulfate are microbial sulfate reduction and sulfate derived from Messinian calcium sulfates.

Oxygen Isotopes

The oxygen isotopic composition of residual sulfate was measured for selected interstitial waters from Sites 974, 975, 977, and 979 (Table 3). The dissolved sulfate was generally enriched in ^{18}O with respect to modern Mediterranean seawater sulfate ($\delta^{18}O[SO_4^{2-}] \approx$

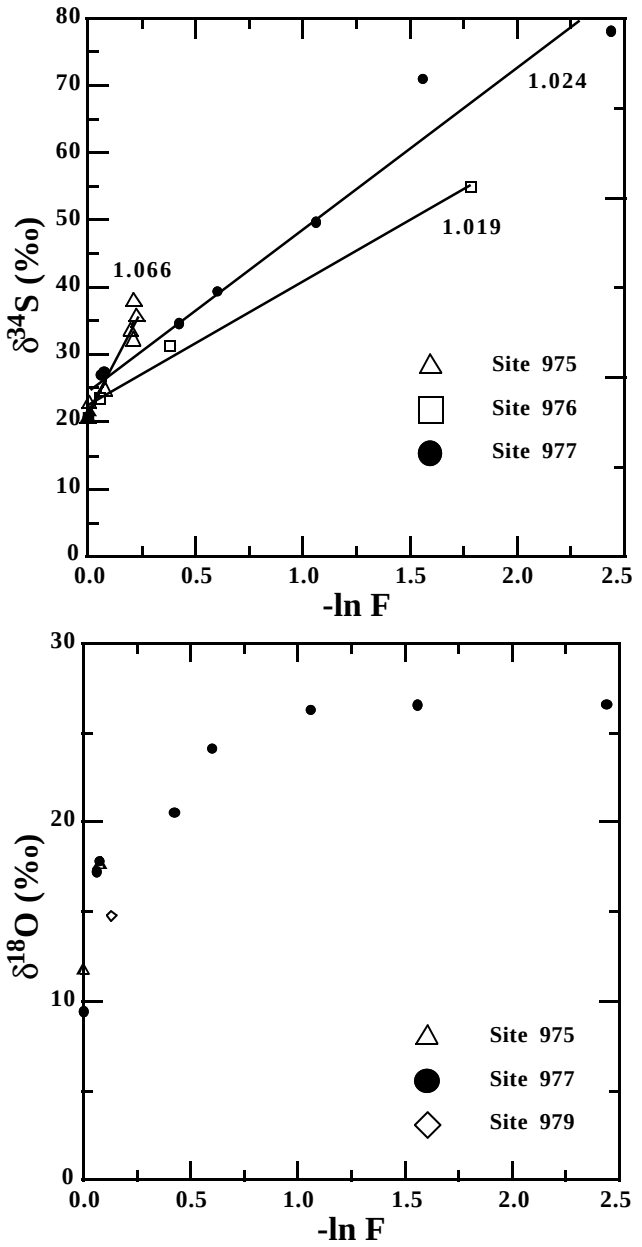

Figure 4. Values of $\delta^{34}S$ and $\delta^{18}O$ of residual sulfate at Sites 975 (down to 47 mbsf), 976, 977, and 979 as a function of the natural logarithm of the residual sulfate fraction of original sulfate remaining (F). Numbers are sulfur isotope fractionation factors calculated from the regression lines (see text).

+9.4‰; Cortecci, 1974a, 1974b), and the values of $\delta^{18}O(SO_4^{2-})$ increase with depth (Fig. 6). Although, the $\delta^{18}O(SO_4^{2-})$ values increase with increasing $\delta^{34}S$ values, the oxygen isotopic composition of the residual sulfate tends to approach an asymptotic value (Fig. 7). For the pore waters of the upper few tens of meters of the profiles, the $\delta^{18}O(H_2O)$ values range between +1.1‰ and +1.5‰ (Table 2). Because of early diagenetic reactions, the values decrease slightly with depth. Water temperatures of 16°, 12°, 15°, and 11°C were measured at Sites 974, 975, 977, and 979 at ~22 mbsf (Comas, Zahn, Klaus, et al., 1996) and increased further downcore. At ~50 mbsf, for instance, temperatures of 17° (Site 977) and 14°C (Site 979) were found, respectively (Comas, Zahn, Klaus, et al., 1996). Using 15°C as a typical water temperature in the sediment sections analyzed for $\delta^{18}O(SO_4^{2-})$, the isotopic composition of dissolved sulfate in equilibrium with interstitial waters of +1.3‰ composition should be +32.4‰ when compared to the extrapolated results from hydrothermal inorganic exchange experiments (Mizutani and Rafter, 1969). Consideration of a range of temperatures between 10° and 20°C leads to theoretical boundary values for the equilibrium isotope composition of dissolved sulfate of +31.2‰ and +33.7‰ (Mizutani and Rafter, 1969). The observed stable isotope data are generally below the proposed equilibrium value (Figs. 6, 7).

Table 2. Stable oxygen isotopes in pore waters and pore water sulfates from Leg 161.

Core, section	Depth (mbsf)	$\delta^{18}O(H_2O)$ (‰)	$\delta^{18}O(SO_4^{2-})$ (‰)
161-974B-			
1H-3	4.45	+1.14	+12.9
2H-3	10.95	+1.04	+15.9
3H-3	20.45	+1.02	+19.3
4H-3		+0.79	—
161-975B-			
1H-1	1.45	+1.38	+11.7
2H-1	5.55	—	+17.6
2H-4	10.05	+1.50	—
21X-3	190.85	+0.17	+24.4
33X-3	306.85	–0.60	+22.0
161-977A-			
1H-1	1.45	+1.48	+17.2
1H-2	2.95	—	+17.8
2H-2	6.88	+1.36	+20.5
2H-4	9.88	—	+24.1
3H-3	17.95	+1.42	+26.2
4H-3	27.45	—	+26.5
5H-3	36.95	+1.35	+26.6
6H-3	46.45	+1.38	—
161-979A-			
2H-3	5.95	+1.31	+14.8
4H-3		+1.32	—
6H-3		+1.23	—

Note: Intervals correspond to Table 1. — = not determined.

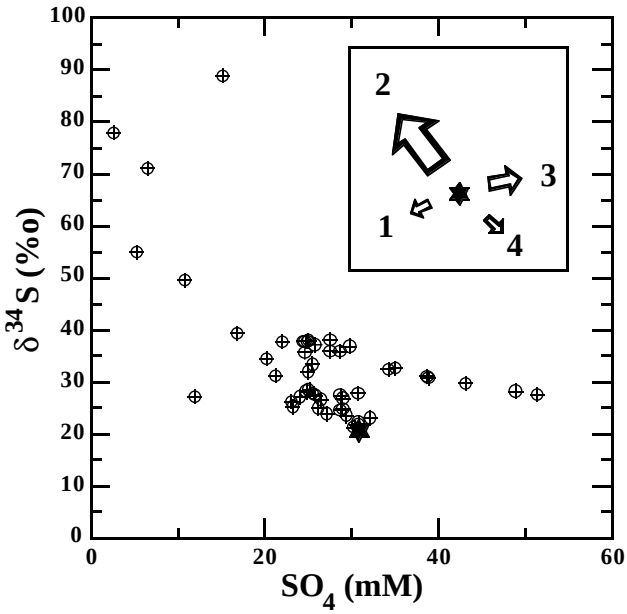

Figure 5. Values of $\delta^{34}S$ vs. concentration of residual sulfate of all measured pore waters from Site 161 and a schematic diagram showing how different processes may influence the composition of dissolved sulfate. Arrows are theoretical trends starting with Mediterranean seawater (star = surface seawater at Site 973) for (1) authigenic precipitation of gypsum, (2) microbial sulfate reduction, (3) dissolution of Messinian gypsum, and (4) reoxidation of dissolved sulfide. Note that the direction of the gypsum dissolution arrow may change when other initial values for the solution are considered. Arrow sizes indicate the estimated overall importance for the Leg 161 pore waters.

Table 3. Stable sulfur isotopes of solids from Hole 975B.

Core, section, interval (cm)	Depth (mbsf)	$\delta^{34}S$ (‰)	Comments
161-975B-			
33X-3, 30-31	305.70	22.8	Gypsum
33X-CC, 6-7	306.92	20.4	Gypsiferous chalk
33X-CC, 14-15	307.00	22.0	Gypsum
33X-CC, 28-29	307.14	22.7	Gypsum
34X-1, 73-74	310.73	22.4	Gypsum
34X-1, 117-118	311.18	22.4	Gypsum
34X-2, 16-17	311.66	22.3	Gypsum
34X-2, 70-71	312.20	22.1	Gypsum
34X-3, 44-45	313.41	22.7	Gypsum
34X-3, 71-72	313.68	22.7	Gypsum, white
34X-3, 71-72	313.68	23.0	Gypsum, gray
34X-CC, 20-21	313.93	21.7	Gypsiferous chalk, light gray
34X-CC, 20-21	313.93	19.5	Gypsiferous chalk, dark gray

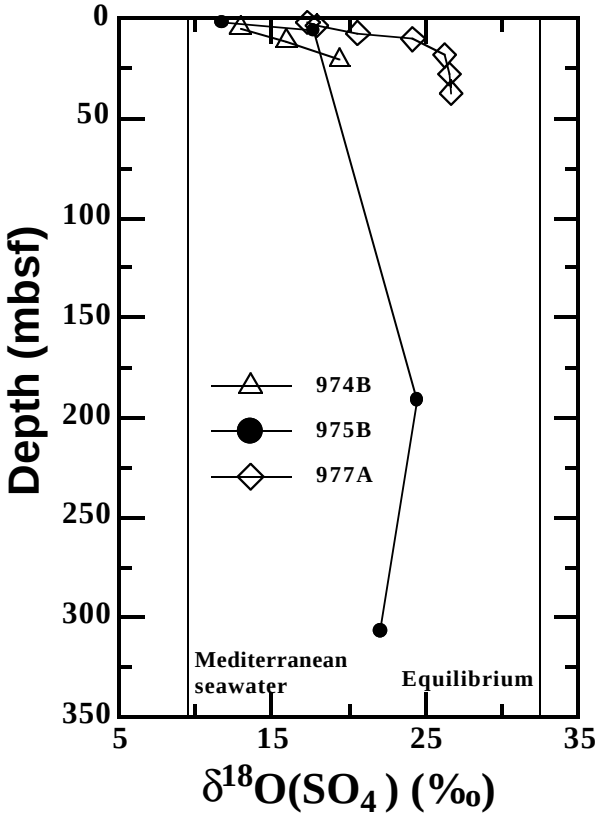

Figure 6. Downhole variations of $\delta^{18}O$ of the residual sulfate from Holes 974B, 975B, and 977A.

The inorganic oxygen isotope exchange reaction between dissolved sulfate and water at low temperatures and neutral pH is extremely slow (e.g., Chiba and Sakai, 1985; Mizutani and Rafter, 1969), and has been found to be negligible in oxic deep-sea sediments up to 50 m.y. old (Zak et al., 1980). However, significant oxygen isotope variations in dissolved sulfate have been observed in microbial sulfate reduction studies (e.g., Mizutani and Rafter, 1973; Fritz et al., 1989) and pore waters of anoxic sediments (Zak et al., 1980; Böttcher et al., 1998; M. E. Böttcher, unpubl. data). In the initial stage of sulfate reduction, kinetic isotope effects are expected to be responsible for a common increase in ^{18}O and ^{34}S values because the ^{32}S-^{16}O bonds are weaker than the ^{34}S-^{16}O and ^{32}S-^{18}O bonds (Zak et al., 1980). From Figure 4, it is evident that the variation of $\delta^{18}O(SO_4^{2-})$ values as a function of ln F does not fall on a linear trend, as expected for an unidirectional kinetic isotope fractionation. As outlined by Böttcher et al. (1998), this difference is caused mainly by oxygen isotope exchange reactions with the aqueous solution via a sulfate-enzyme complex, which is formed as an intermediate reaction product (Fritz et al., 1989), leading to an increased equilibration between residual sulfate and pore water with increasing degree of microbial sulfate reduction. Figure 7 shows that the oxygen isotope data of pore-water sulfate increase more rapidly than the $\delta^{34}S$ values increase at Sites 974 and 975 compared to Site 977. This is caused by lower sulfate reduction rates at Sites 974 and 975 (Fig. 3), which enables a more intense oxygen isotope exchange upon reaction even at low degrees of sulfate reduced. The distinct relationships between $\delta^{18}O$ and $\delta^{34}S$ values seem to be related to their different sulfate reduction rates, thus confirming the previous suggestion of Böttcher et al. (1998) that different sulfate reduction rates in marine sediments are directly reflected by $\delta^{18}O$–$\delta^{34}S$ plots.

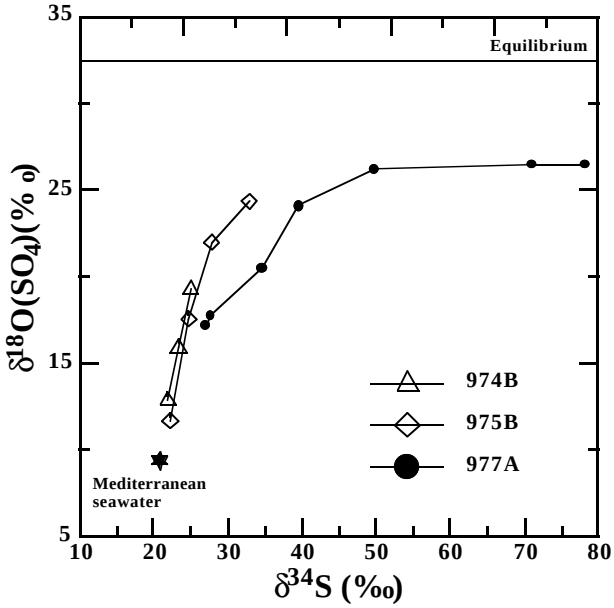

Figure 7. Values of $\delta^{34}S$ vs. $\delta^{18}O$ of residual sulfate from Holes 974B, 975B, and 977A.

The decrease in $\delta^{18}O(SO_4^{2-})$ at greater depth at Site 975 (Fig. 6) results from the dissolution of upper Miocene evaporites with an approximate oxygen isotope value of +16‰ (Stenni and Longinelli, 1990). The slight depletion of the interstitial water in ^{18}O at greater depth, which is caused by some diagenetic water-rock interactions (Bernasconi, Chap. 33, this volume), should only have been a minor influence on the composition of dissolved sulfate. The oxygen isotope data of dissolved sulfate for Site 977 level off below the theoretical equilibrium value of +32.4‰. This observation is similar to the experimental results of Fritz et al. (1989), in which a smaller isotope fractionation was observed at steady state probably results from an uncertainty in the values.

Carbon Isotopes

The carbon isotopic compositions of dissolved inorganic carbonate species at Sites 974, 975, 976, 977, and 979 vary between –0.1‰ and –22.6‰ relative to V-PDB (Table 1). The downcore profiles of all sites show similar trends. Specifically, in the uppermost part of the sediments, at depths at or above 50 mbsf, observed minima in the $\delta^{13}C$ records probably result from the microbial degradation of organic matter by sulfate-reducing bacteria and the concomitant liberation of CO_2. The extent of ^{13}C depletion in dissolved inorganic carbonate species at the minima is directly related to the amount of sulfate reduced (Figs. 2, 8). The subsequent increase in $\delta^{13}C$ of dissolved inorganic carbonate species with increasing depth at Sites 976, 977, and

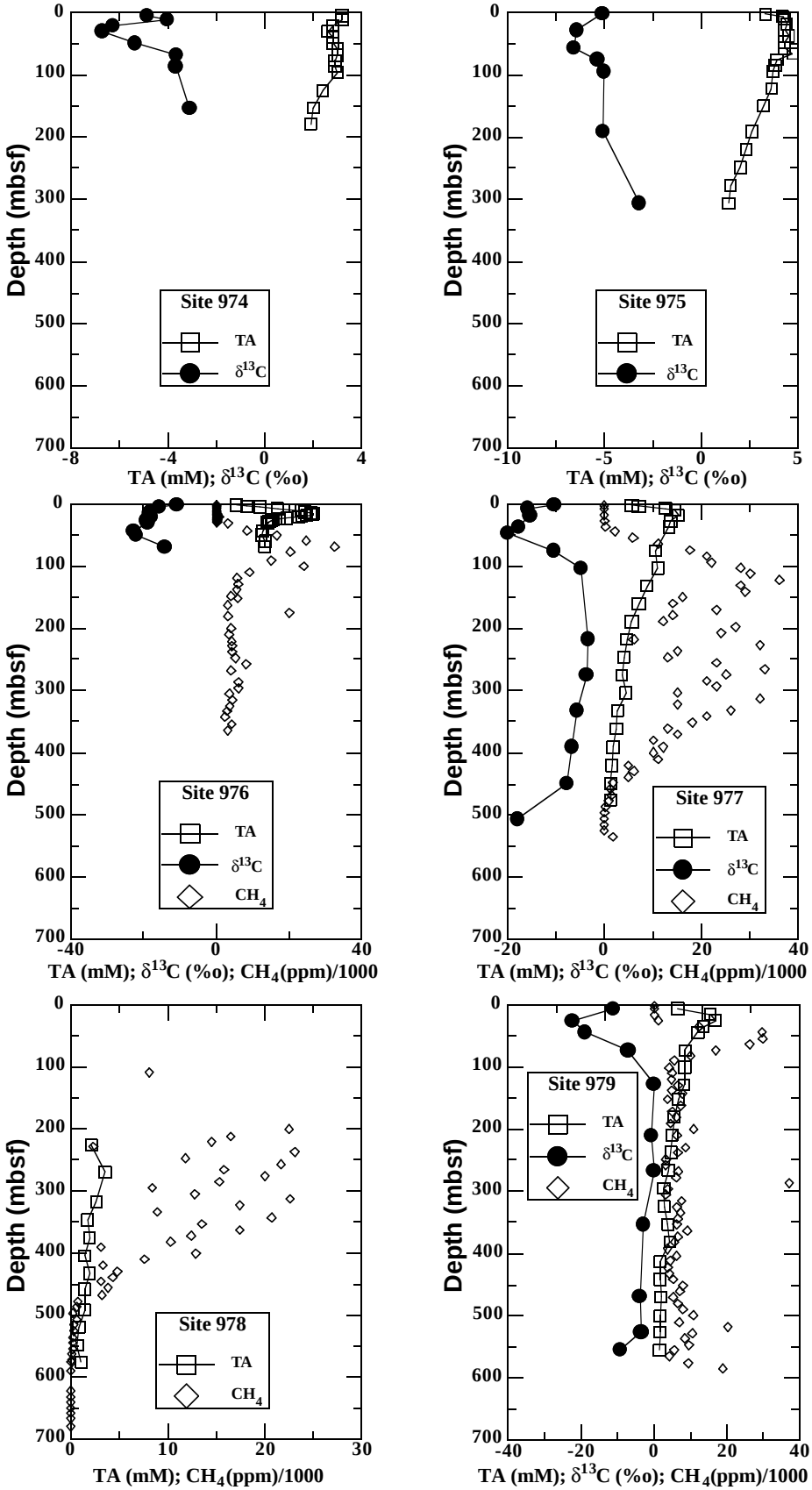

Figure 8. Profiles of pore-water alkalinity (TA) concentration and $\delta^{13}C$ of dissolved inorganic carbonate species vs. depth for Sites 974–979. Superimposed headspace methane concentrations for Sites 976–979 are from Comas, Zahn, Klaus, et al. (1996).

979 is caused by bacterial methanogenesis, which succeeds sulfate reduction in anaerobic organic carbon-rich sediments and is clearly reflected by the variation of measured headspace methane concentrations (Fig. 8). Because the activity of methane-producing bacteria leads to the formation of methane enriched in ^{12}C (Games et al., 1978; Carothers and Kharaka, 1980; Botz et al., 1997), the interstitial water can become enriched in ^{13}C, and the pore waters evolve to higher $\delta^{13}C$ values as bacterial methane formation continues.

The decrease of $\delta^{13}C$ in the deepest intervals of Sites 977 and 979 (Fig. 8) is probably related to a repeated onset of microbial activity oxidizing organic matter or methane. At least for Site 977, the increased availability of dissolved sulfate indicates that sulfate may act again as the electron acceptor. Probably, the lowermost pore-water sample analyzed at Site 979 became completely depleted in sulfate because of microbial sulfate reduction, and sulfate is expected to increase in the underlying sediments.

It should be noted, however, that the variations of dissolved calcium and magnesium (Comas, Zahn, Klaus, et al., 1996; Bernasconi, Chap. 33, this volume) and alkalinity with depth (Fig. 8) also provide evidence for an influence on the isotopic composition of dissolved inorganic carbonate species by carbonate dissolution and precipitation reactions. The downcore increase of $\delta^{13}C$ values at Sites 974 and 975 can only be related to carbonate diagenesis, because the high dissolved sulfate concentrations hindered methanogenesis (e.g., Carothers and Kharaka, 1980).

CONCLUSIONS

The variation of concentration and stable isotopic compositions ($\delta^{34}S$, $\delta^{18}O$) of dissolved sulfate and $\delta^{13}C$ of inorganic carbonate species in interstitial waters from the western Mediterranean are dominated by the following processes:

1. Microbiological degradation of organic matter and related sulfate reduction in the upper sediment column;
2. Dissolution of gypsum (Site 975);
3. Dissolved sulfate derived from saline evaporite brines (Sites 974 and 978);
4. Generation of methane by in situ fermentation of organic matter (Sites 976–979);
5. Dissolution and precipitation of carbonate minerals; and
6. Oxidation of methane (Sites 977 and 979?).

Sulfur and oxygen isotope measurements on the dissolved sulfate of interstitial waters from the western Mediterranean are shown to be a powerful tool in the evaluation of sinks, sources, and microbiological transformation reactions during sediment diagenesis. A previous suggestion is confirmed that different sulfate reduction rates in marine sediments are directly reflected in $\delta^{18}O$–$\delta^{34}S$ plots.

ACKNOWLEDGMENTS

We thank the scientific and technical crew of Leg 161 and R. Wehausen for support during sampling. We further acknowledge the oxygen isotope measurements on sulfate by J. Szaran and S. Halas (University of Lublin) and thank R. Botz for a preprint of his publication. Musical inspiration by Ornette Coleman and the United Jazz + Rock Ensemble during manuscript preparation was highly appreciated. The study was funded by the German Science Foundation (ODP-SPP). The constructive reviews of T.W. Lyons and J.B. Martin helped to improve the manuscript.

REFERENCES

Berner, R.A., 1980. *Early Diagenesis: A Theoretical Approach:* Princeton, NJ (Princeton Univ. Press).

Borowski, W.S., Paull, C.K., and Ussler, W., III, 1996. Marine pore-water sulfate profiles indicate in situ methane flux from underlying gas hydrate. *Geology,* 24:655–658.

Böttcher, M.E., Brumsack, H.-J., and De Lange, G.J., 1998. Sulfate reduction and related stable isotope (^{34}S, ^{18}O) variations in interstitial waters from the eastern Mediterranean. *In* Robertson, A.H.F., Emeis, K.-C., Richter, C., and Camerlenghi, A. (Eds.), *Proc. ODP, Sci. Results,* 160: College Station, TX (Ocean Drilling Program), 365–373.

Böttcher, M.E., Rusch, A., Höpner, T., and Brumsack, H.-J., 1997. Stable sulfur isotope effects related to local intense sulfate reduction in a tidal sandflat (Southern North Sea): results from loading experiments. *Isot. Environ. Health Stud.,* 33:453–473.

Böttcher, M.E., and Usdowski, E., 1993. $^{34}S/^{32}S$ ratios of the dissolved sulphate of river, well and spring waters in a gypsum-carbonate karst area at the southwest edge of the Harz mountains. *Z. Dtsch. Geol. Ges.,* 144:471–477.

Botz, R., Pokojski, H.-D., Schmitt, M., and Thomm, M., 1997. Carbon isotope fractionation during the bacterial methanogenesis by CO_2 reduction. *Org. Geochem.,* 25:255–262.

Burdett, J.W., Arthur, M.A., and Richardson, M., 1989. A Neogene seawater sulfur isotope age curve from calcareous pelagic microfossils. *Earth Planet. Sci. Lett.,* 94:189–198.

Canfield, D.E., 1991. Sulfate reduction in deep-sea sediments. *Am. J. Sci.,* 291:177–188.

Canfield, D.E., and Teske, A., 1996. Late Proterozoic rise in atmospheric oxygen concentration inferred from phylogenetic and sulfur-isotope studies. *Nature,* 328:127–132.

Carothers, W.W., and Kharaka, Y.K., 1980. Stable carbon isotopes of HCO_3^- in oil-field waters: implications for the origin of CO_2. *Geochim. Cosmochim. Acta,* 44:323–332.

Chambers, L.A., and Trudinger, P.A., 1979. Microbiological fractionation of stable sulfur isotopes: a review and critique. *Geomicrobiol. J.,* 1:249–293.

Chiba, H., and Sakai, H., 1985. Oxygen isotope exchange rate between dissolved sulfate and water at hydrothermal temperatures. *Geochim. Cosmochim. Acta,* 49:993–1000.

Comas, M.C., Zahn, R., Klaus, A., et al., 1996. *Proc. ODP, Init. Repts.,* 161: College Station, TX (Ocean Drilling Program).

Cortecci, G., Molcard, R., and Noto, P., 1974. Isotopic analysis of the deep structure in the Tyrrhenian Sea. *Nature,* 250:134–136.

Cortecci, G., Noto, P., and Molcard, R., 1974. Tritium and sulfate-oxygen isotopes in Mediterranean Sea: some profiles in the low Tyrrhenian Basin. *Bull. Geofis. Teor. Appl.,* 16:292–298.

De Lange, G.J., Boelrijk, N.A.I.M., Catalano, G., Corselli, C., Klinkhammer, G.P., Middelburg, J.J., Mueller, D.W., Ullman, W.J., Van Gaans, P., and Woittiez, J.R.W., 1990. Sulphate-related equilibria in the hypersaline brines of the Tyro and Bannock Basins, eastern Mediterranean. *Mar. Chem.* 31:89–112.

Fritz, P., Basharmal, G.M., Drimmie, R.J., Ibsen, J., and Qureshi, R.M., 1989. Oxygen isotope exchange between sulphate and water during bacterial reduction of sulphate. *Chem. Geol. (Isot. Geosc. Sec.),* 79:99–105.

Games, L.M., Hayes, J.M., and Gunsales R.P., 1978. Methane-producing bacteria: natural fractionations of the stable carbon isotopes. *Geochim. Cosmochim. Acta,* 42:1295–1297.

Gieskes, J.M., Gamo, T., and Brumsack, H., 1991. Chemical methods for interstitial water analysis aboard *JOIDES Resolution.* ODP Tech. Note, 15.

Gonfiantini, R., Stichler, W., and Rozanski, K., 1995. Standards and intercomparison materials distributed by the International Atomic Energy Agency for stable isotope measurements. *IAEA-TECDOC*-825, 13–29.

Hartmann, M., and Nielsen, H., 1969. $\delta^{34}S$-Werte in rezenten Meeressedimenten und ihre Deutung am Beispiel einiger Sedimentprofile aus der westlichen Ostsee. *Geol. Rundsch.,* 58:621–655.

Jørgensen, B.B., 1979. A theoretical model of the stable sulfur isotope distribution in marine sediments. *Geochim. Cosmochim. Acta,* 43:36–74.

Manheim, F.T., and Sayles, F.L., 1974. Composition and origin of interstitial waters of marine sediments, based on deep sea drill cores. *In* Goldberg, E.D. (Ed.), *The Sea* (Vol. 5): *Marine Chemistry: The Sedimentary Cycle:* New York (Wiley), 527–568.

Mizutani, Y., 1971. An improvement of the carbon-reduction method for the oxygen isotopic analysis of sulphates. *Geochem. J.*, 5:69–77.

Mizutani, Y., and Rafter, T.A., 1969. Oxygen isotopic composition of sulphates—part 3: Oxygen isotopic fractionation in the bisulphate ion-water system. *N.Z. J. Sci.*, 12:54–59.

————, 1973. Isotopic behaviour of sulphate oxygen in the bacterial reduction of sulphate. *Geochem. J.*, 6:183–191.

Rees, C.E., 1973. A steady state model for sulfur isotope fractionation in bacterial reduction processes. *Geochim. Cosmochim. Acta*, 37:1141–1162.

Stenni, B., and Longinelli, A., 1990. Stable isotope study of water, gypsum and carbonate samples from the Bannock and Tyro Basins, Eastern Mediterranean. *Mar. Chem.*, 31:123–135.

Sweeney, R.E., and Kaplan, I.R., 1980. Diagenetic sulfate reduction in marine sediments. *Mar. Chem.*, 21:165–174.

Thode, H.G., and Monster, J., 1965. Sulfur isotope geochemistry of petroleum, evaporites and ancient seas. *In* Fluids in Subsurface Environments, *AAPG Mem.*, 4:367–377.

Zak, I., Sakai, H., and Kaplan, I.R., 1980. Factors controlling the $^{18}O/^{16}O$ and $^{34}S/^{32}S$ isotope ratios of ocean sulfates, evaporites and interstitial sulfates from modern deep sea sediments. *In* Goldberg, E.D., Horibe, Y., and Saruhashi, K. (Eds.), *Isotope Marine Chemistry:* Tokyo (Rokakuho), 339–373.

Date of initial receipt: 9 May 1997
Date of acceptance: 20 January 1998
Ms 161SR-229